DOI:http://dx.doi.org/10.18524/1810-4215.2020.33.216289

SPECTROSCOPIC INVESTIGATIONS OF THE POLARIS (α UMi) SYSTEM: RADIAL VELOCITY MEASUREMENTS, NEW ORBIT, AND COMPANION INFLUENCE FOR THE CEPHEID POLARIS Aa PULSATION ACTIVITY.

I. A. Usenko,[1,2] A. S. Miroshnichenko,[3,4,5] S. Danford,[3] V. V. Kovtyukh,[1] D. G. Turner[6]

[1] Astronomical Observatory, Odessa National University, Shevchenko Park, Odessa 65014, Ukraine, *vkovtyukh@ukr.net*
[2] Mykolaiv Astronomical Observatory, Obsevatorna 1, Mykolaiv 54030, Ukraine, *igus99@ukr.net*
[3] Dept. of Physics and Astronomy, University of North Carolina at Greensboro, P.O. Box 261170, Greensboro, NC 27402, USA, *a_mirosh@uncg.edu; danford@uncg.edu*
[4] Main Astronomical Observatory of the Russian Academy of Sciences, Pulkovskoe shosse 65–1, Saint-Petersburg, 196140, Russia
[5] Fesenkov Astrophysical Institute, Observatory 23, Almaty, 50020, Kazakhstan
[6] Dept. of Astronomy and Physics, Saint Mary's University 923 Robie Street, Halifax B3H3C3, Nova Scotia, Canada, *turner@ap.smu.ca*

ABSTRACT. Thirty three spectra of the Polaris system obtained in August–December 2019 and February–April 2020 at the 0.81 m telescope of the Three College Observatory (TCO, North Carolina, USA) were used to determine the radial velocities (RV) and effective temperature of the Cepheid Polaris Aa. These new data have been added to the entire Polaris system RV data collection (over 2,500 measurements) to compute a new orbit of the Polaris Aa companion. Furthermore we have used our eight observational datasets taken in 2015–2020 and eight datasets taken in 2011–2018 by Anderson (2019) to check for possible influence of the orbital motion of Polaris Ab on the Polaris Aa pulsational activity. It was found that the mean pulsational period in 2015–2020 was quite stable (3.976±0.012 days), while the pulsational amplitude showed evident changes: a growth before HJD 2457350 with a following decrease. This fact could be due to the Polaris Ab passing through the periastron.

Key words: α UMi (Polaris Aa and Polaris Ab) system: radial velocities; Polaris Aa effective temperatures; Polaris Aa pulsational period and amplitude; orbital elements.

АНОТАЦІЯ. Тридцять три спектри системи Полярної, отримані в серпні-грудні 2019 та лютому-квітні 2020 рр. на 0.81-м телескопі Обсерваторії Трьох Колледжів (ТСО, Північна Кароліна, США) були використані для отримання радіальних швидкостей та ефективних температур цефеїди Полярної Aa. Ці нові данні були додані до загальної колекції радіальної швидкості Полярної (більш ніж 2500 оцінок), щоб розрахувати нову орбіту супутника цефеїди – Полярної Ab. Усі наші 187 спектри, що були отримані за період 2015–2020 рр. у восьми спостережних серіях за додатком восьми серій 2011–2018 рр. з роботи Андерсона (2019, 164 спектра) були використан, щоб перевірити можливий вплив орбітального руху Полярної Ab на пульсаційну активність Полярної Aa. Цей спостережний період є цікавим, тому що він охоплює час проходження через періастр та висхідний вузол супутника Полярна Ab. Було встановлено, що середній пульсаційний період у 2015–2020 рр. був досить стабільним (3.9722±0.001 діб), тоді як амплітуда пульсації показує наявні зміни: зріст до HJD 2457350 з наступним зменьшенням. Ций факт може бути пояснений проходженням Полярної Ab через періастр орбіти. Згідно з поведінкою пульсаційної амплітуди, ми можемо передбачити її поведінку у найближчому майбутньому. У зв'язку з цим, подальші отримання радіальних швидкостей системи Полярної А мають дуже важливе значення. Орбітальний рух зорі Полярнної Ab має вплив на пульсаційну амплітуду Полярної Aa в залежності від орбітальної фази. А середня ефективна температура цефеїди Полярної Aa показує помітний зріст за кожний спостережній

сезон.

Ключові слова: Класичні цефеїди; система α UMi (Полярна Aa та Полятна Ab) : Радіальні швидкості руху; Ефективні температури Полярної Aa; Пульсаційний період і амплітуда Полярної Aa ; Елементи орбіти.

1.Introduction

Radial velocity measurements of the Polaris system, in addition to studies of its pulsation period changes and the amplitude of the pulsation curve of the main component, the Cepheid Polaris Aa, are important for clarifying the properties of the Polaris Ab companion and the dynamics of this binary system. Over 2,500 RV estimates that cover four orbital cycles of Polaris Ab have been obtained in the last about 130 years (see Fig. 1).

The first orbital cycle (HJD 2414900 – 2426000) is the most covered compared to the second one (HJD 2426000 – 2436500), while the third cycle is the least covered. The observations taken between HJD 2445000 and 2447500 were carried out quite frequently. These data were obtained with photographic plates. A large fraction of the most recent observations taken during the fourth covered orbital cycle (since HJD 2447500) was obtained with CCD detectors.

An abrupt decrease of the pulsation amplitude is clearly visible in Fig. 1. It had began precisely in the "third orbit" time lag, especially near the ascending node of the orbit. Since the orbital motion of Polaris Ab is retrograde (Evans et al. 2018), the moment of its periastron passage occurs before passing through the point of the ascending node. It can be noted that no frequent spectroscopic observations were reported between 2007 and 2011 except for a few measurements. Our observations between 2015 and 2018 (Usenko et al. 2016, 2017, 2018) and those presented by Anderson (2019) were taken around these important orbital phases (see Fig. 2).

Additionally, according to our estimates, the pulsation period of Polaris Aa has increased compared to that of 2016–2017, and the pulsation amplitude showed a tendency to decrease (Usenko et al. 2018). However, Anderson (2019) indicates an amplitude constancy in 2011–2018. In this regard, the question arises: what are the roles of the orbital configuration and the orbital motion itself in changing the Polaris Aa pulsation amplitude?

To answer this question, we carried out further spectroscopic observations of the Polaris system from August 2018 to April 2020 and analyzed the results of the RV measurements relative to the orbital system's motion. In particular, the following goals were set:

1. To choose short-term data sets (from 10 to 150 days) during which RV changes due to orbital motion could be neglected.

2. To obtain the best purely sinusoidal approximation for each of these data sets and to determine parameters of every orbit/pulsational cycle (period, amplitude, mean heliocentric velocity and the cycle's initial phase).

3. To determine the mean heliocentric velocity values (γ-velocity) to calculate the orbit of Polaris system.

4. To subtract the orbital velocity values from the estimated heliocentric velocity ones.

5. To derive the pulsational cycle parameters from all our measurements.

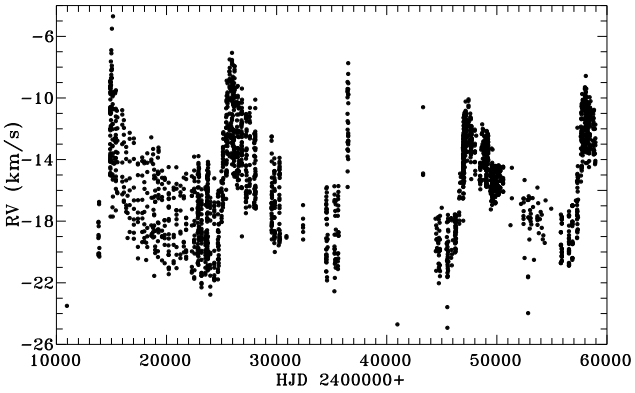

Figure 1: Polaris radial velocity estimations over the last ∼130 years.

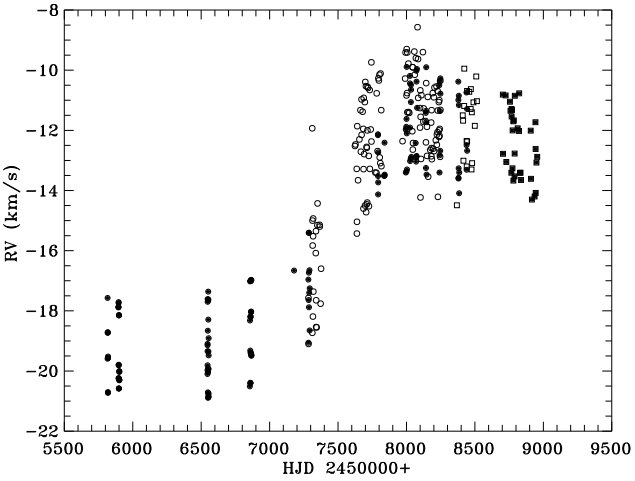

Figure 2: Radial velocity measurements of Polaris Aa from 2011 to 2020. Data from Anderson (2019) are shown by filled circles, our data obtained from 2015 to the first half of 2018 (open circles), September 2018 – January 2019 (open squares), second half of 2019 – first half 2020 (filled squares).

Therefore we have used eight our observational sets, eight sets from Anderson (2019) data, and some earlier sets for a more precise determination of the Polaris system orbital period. The Kamper (1996) data were omitted due to a very small pulsational amplitude at that time period.

2. Observations and development of spectra

Fifty three spectra were obtained in the present data set: 20 in September 2018–January 2019, 24 in August–December 2019, and 9 in February–April 2020. All the observations were obtained with the 0.81 m telescope of the Three College Observatory (TCO) in North Carolina. This telescope is equipped with an échelle spectrograph manufactured by Shelyak Instruments [1]. The instrument operates in the spectral range from 3850 to 7900 Å with a spectral resolving power of $R \sim$ 12,000 and no gaps the between spectral orders. The average S/N ratio in the continuum was 150–200, while most spectral lines used in our analysis were taken from the range 4900–6800 Å. The data were reduced with the *échelle* package in IRAF.

The DECH 30 software package[2] was used to measure the line depths and RVs. The latter were measured by cross-correlation and the parabolic fitting methods. The uncertainty of the RV measurements is between 1.0 and 1.8 $\mathrm{km\,s^{-1}}$. The line depths were used to determine the effective temperature. A method based on the depth ratios of selected pairs of spectral lines is the most sensitive to the temperature (Kovtyukh 2007). The method provides an internal accuracy of the $T_{\rm eff}$ determination of ∼10–30 K (standard deviation of the average).

The derived values of $T_{\rm eff}$ and RV measured from hydrogen and metallic lines in each spectrum are presented in Table 1. These RV values are shown in Fig. 2.

3. Pulsation and orbital period analysis

The next step in the analysis was to use purely sinusoidal approximations for the data sets determined by the least squares method. As an example, one of these approximations is shown in Fig. 3, and the best-fit parameters are presented in Table 2. To derive a more precise orbital period of the Polaris A system, we have used the data from our observational seasons in combination with those from eight seasons published by Anderson (2019) and from six seasons published by Roemer (1965). The following general equation for the RV variations on an elliptical orbit was used for finding the best fits to the data:

[1] http://www.shelyak.com
[2] http://www.gazinur.com/DECH-software.html

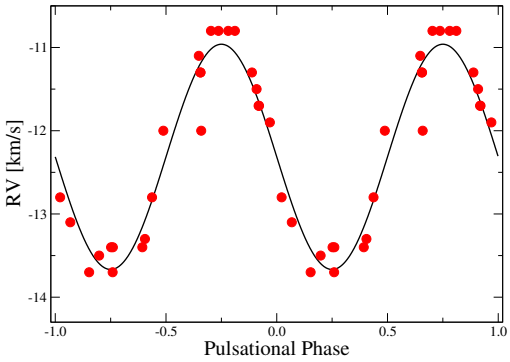

Figure 3: A sinusoidal least square method approximation for our HJD 2458704–2458837 observational set.

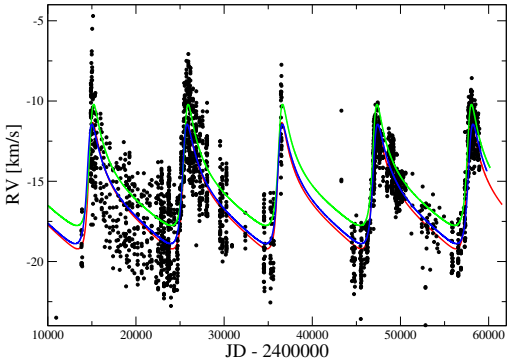

Figure 4: Comparison of the Polaris orbits: red line – Kamper (1996), green line – Anderson (2019), blue line – our data.

$$RV = \gamma + K(e\ cos\ \omega + cos(M + \omega)), \qquad (1)$$

where K is the semi-amplitude of radial velocity variations, γ is the systemic RV, e is the orbital eccentricity (was always set to zero), ω - the argument of the periastron, M is the true anomaly.

Table 3 contains the orbital parameters of the Polaris system that had been published earlier and our new results. Figure 4 represents the median orbital RV curves of the Polaris A system using the orbital elements from Anderson (2019), Kamper(1996), and this work that have been calculated according to a selection of observational seasons from Table 2 and the data from Table 1. As seen from Table 3 and Fig. 4, our results are closer to those found by Kamper (1996). According to the orbital elements form Anderson (2019), Polaris Ab passed through periastron on 29 November 2016 and through the ascending node - on 18 October 2017, while using the elements from Kamper (1996) these dates are 1 April 2017 and 17 April 2018, respectively.

Figure 5 shows the pulsational period changes according to Anderson (2019) and to our data. As seen, these changes show some periodicity. If we use all our RV data with the orbital velocity subtracted, then we have a Fourier power spectrum (Fig. 6) with quite a

Table 1: Observational data of α UMi (NL – number of lines)

HJD	$T_{\rm eff}$	σ	Phase	RV($\mathrm{km\,s^{-1}}$)					
2450000+	K	K		Metals	σ	NL	H_α	H_β	H_γ
8368.5931	6058	21	0.934	–14.49	1.70	176	–14.45	–14.84	–14.67
8411.4928	6057	20	0.731	–11.50	1.77	159	–12.23	–9.93	–8.58
8413.5843	6055	19	0.258	–11.68	1.68	189	–12.23	–8.92	–10.96
8416.5683	6073	23	0.009	–13.01	1.61	173	–13.42	–7.80	–11.84
8421.6551	5984	18	0.289	–11.19	1.78	166	–11.20	–7.53	–10.24
8422.6439	5969	21	0.538	–9.95	1.86	157	–9.47	–4.03	–8.90
8439.6274	6038	22	0.812	–12.35	1.69	147	–12.07	–9.87	–11.31
8440.6117	6086	21	0.060	–13.20	1.91	155	–13.40	–10.75	–12.20
8442.6074	6050	21	0.562	–10.69	1.86	163	–10.18	–6.94	–8.58
8443.6292	6117	23	0.819	–12.37	1.60	153	–13.25	–8.88	–11.26
8458.6511	6074	21	0.600	–10.72	1.48	158	–11.30	–8.21	–8.81
8469.5308	6007	21	0.338	–11.29	1.47	159	–10.92	–8.52	–9.70
8470.5557	6083	25	0.596	–10.63	1.59	164	–10.74	–6.97	–9.46
8475.5715	6095	24	0.859	–13.30	1.20	161	–14.05	–9.15	–11.57
8477.5626	5948	20	0.360	–11.40	1.34	159	–10.33	–8.56	–9.44
8479.5699	6102	22	0.865	–13.09	1.45	170	–13.39	–10.70	–12.34
8489.5582	6041	20	0.379	–11.07	1.51	164	–10.38	–7.44	–9.77
8499.5614	6090	22	0.897	–11.85	1.37	160	–11.89	–8.81	–10.80
8509.5801	6050	22	0.418	–10.21	1.46	171	–10.12	–7.02	–8.83
8514.6088	6042	27	0.684	–11.03	1.63	170	–11.47	–9.57	–9.53
8704.6331	6011	20	0.557	–10.81	1.30	172	–10.82	–8.18	–10.98
8705.5884	6073	24	0.798	–12.78	1.30	164	–12.85	–11.23	–13.38
8724.5957	6058	19	0.588	–10.84	1.32	171	–10.43	–7.25	–10.49
8729.5863	6072	20	0.846	–13.05	1.38	181	–13.91	–8.96	–12.10
8755.7058	5931	23	0.429	–11.05	1.43	161	–11.09	–7.48	–10.23
8760.6257	6158	27	0.669	–11.35	1.52	164	–11.37	–9.05	–10.88
8766.6023	6032	29	0.176	–13.41	1.40	163	–14.03	–10.60	–12.85
8767.6403	6009	22	0.437	–11.29	1.26	164	–11.17	–7.81	–11.16
8768.6482	5985	26	0.691	–11.54	1.23	160	–11.54	–8.85	–11.43
8771.6134	6042	24	0.439	–11.32	1.48	159	–11.28	–8.25	–10.17
8774.5861	6078	23	0.188	–13.26	1.49	163	–14.76	–11.46	–12.86
8775.5933	6086	24	0.442	–12.00	1.29	164	–12.21	–9.79	–11.66
8780.5991	6049	18	0.703	–11.70	1.28	163	–11.95	–9.45	–11.51
8781.5251	6079	25	0.937	–13.67	1.37	158	–15.00	–11.83	–13.99
8784.5618	6078	23	0.702	–11.67	1.33	165	–11.20	–7.97	–10.52
8789.6421	6122	25	0.983	–13.53	1.54	170	–15.50	–12.51	–13.87
8790.5904	6057	25	0.222	–12.77	1.29	159	–14.39	–10.87	–12.06
8791.6463	5999	24	0.488	–10.85	1.46	160	–11.31	–7.85	–9.83
8812.5489	6056	21	0.756	–11.93	1.44	163	–12.30	–9.40	–10.66
8822.5455	6083	23	0.275	–12.02	1.45	168	–13.87	–10.18	–11.67
8823.5373	6050	20	0.525	–10.77	1.30	162	–10.54	–7.66	–9.60
8829.5468	6078	18	0.040	–13.41	1.47	161	–15.32	–11.08	–12.95
8833.5510	6040	26	0.049	–13.41	1.61	163	–15.63	–11.38	–13.32
8837.5157	6159	25	0.049	–13.65	1.62	192	–15.21	–11.81	–13.19
8907.6854	6031	20	0.734	–12.01	1.56	166	–12.26	–9.55	–10.86
8909.6695	6051	23	0.234	–13.61	1.63	196	–14.32	–14.73	–12.94
8916.6189	6121	23	0.986	–14.30	1.43	156	–14.86	–12.14	–13.28
8936.5658	6106	21	0.013	–14.20	1.85	197	–15.00	–11.32	–12.85
8942.5727	6034	22	0.527	–11.73	1.14	157	–11.45	–9.05	–10.31
8943.6633	6079	18	0.802	–12.62	1.17	153	–12.17	–9.44	–11.01
8944.6059	6145	24	0.040	–14.08	1.40	159	–15.15	–11.92	–13.34
8949.6344	6118	29	0.307	–13.07	1.49	157	–14.01	–10.48	–11.38
8955.5861	6100	23	0.807	–12.88	1.47	194	–12.85	–10.62	–11.78

Table 2: Polaris *RV* dataset during our and *HERMES* observational sets.

Source	JD range 2450000+	JD_{mid} 2450000+	NL	Period (days)	γ ($km\,s^{-1}$)	K ($km\,s^{-1}$)	T_0 2450000+ (days)
Roemer	14876−14951	14918	21	3.9585±0.002	−11.92±0.11	3.755±0.18	14874.591±0.025
Roemer	15378−15403	15391	16	3.9098±0.029	−13.27±0.50	2.358±0.79	15374.715±0.171
Roemer	18784−18878	18831	16	3.8087±0.020	−16.84±0.82	2.426±1.20	18778.901±0.292
Roemer	29792−29833	29816	11	4.0371±0.015	−16.79±0.03	2.047±0.15	29787.812±0.073
Roemer	34492−34576	34534	16	3.9847±0.005	−18.41±0.15	2.240±0.23	34488.449±0.054
Roemer	36440−36501	36472	8	3.9323±0.023	−10.75±0.10	2.288±0.13	36434.439±0.038
Hermes1	55816−55901	55872	10	3.9681±0.015	−19.18±0.23	1.466±0.33	55813.885±0.18
Hermes2	56546−56554	56550	9	3.9553±0.004	−19.17±0.02	1.675±0.03	56540.795±0.01
Hermes3	56855−56866	56862	11	3.9586±0.006	−18.73±0.04	1.821±0.05	56850.632±0.02
Hermes4	57283−57293	57288	9	3.9805±0.013	−17.20±0.07	1.829±0.13	57279.526±0.03
Hermes6	57994−58077	58033	22	3.9719±0.003	−11.67±0.08	1.775±0.12	57990.516±0.038
Hermes7	58141−58248	58196	14	3.9719±0.002	−11.77±0.09	1.733±0.13	58137.504±0.047
Hermes8	58379−58439	58402	9	3.9633±0.0028	−12.29±0.05	1.751±0.06	58375.814±0.024
TCO1	57283−57376	57332	21	3.9754±0.011	−16.72±0.41	2.052±0.60	57279.459±0.174
TCO2	57623−57744	57690	37	3.9787±0.009	−12.75±0.40	1.717±0.60	57617.046±0.218
TCO3	57772−57816	57798	12	4.0029±0.016	−11.78±0.17	1.592±0.20	57767.853±0.137
TCO4	57971−58109	58048	29	3.9633±0.004	−11.13±0.23	1.731±0.36	57966.927±0.109
TCO5	58120−58248	58196	38	3.9738±0.008	−11.65±0.24	1.115±0.36	58113.639±0.184
TCO6	58368−58514	58453	18	3.9754±0.005	−11.85±0.23	1.510±0.33	58363.854±0.139
TCO7	58704−58837	58778	24	3.9692±0.007	−12.31±0.20	1.353±0.27	58701.532±0.140
TCO8	58907−58955	58934	9	3.9659±0.007	−12.92±0.10	1.362±0.15	58904.094±0.065

Table 3: Orbital Parameters of Polaris systems.

Parameter	Roemer (1965)	Kamper (1996)	Turner et al. (2007)	Anderson (2019)	This work
P, yrs	30.46±0.10	29.59±0.02	29.71±0.09	29.32±0.13	29.25±0.03
e	0.639±0.012	0.608±0.005	0.543±0.010	0.620±0.008	0.633±0.044
T_0, yr	1928.48±0.08	1928.48±0.08	1928.57±0.06	2016.19±0.1	1987.22±0.1
ω, deg	307.24±1.82	303.01±0.75	309.6±0.7	307.2±2.5	302.5±2.7
K, $km\,s^{-1}$	4.09±0.1	3.72±0.03	4.41±0.07	3.768±0.073	3.93±0.12
γ, $km\,s^{-1}$	−16.41	−16.42±0.03	−15.90±0.06	−15.387±0.04	−16.61±0.12

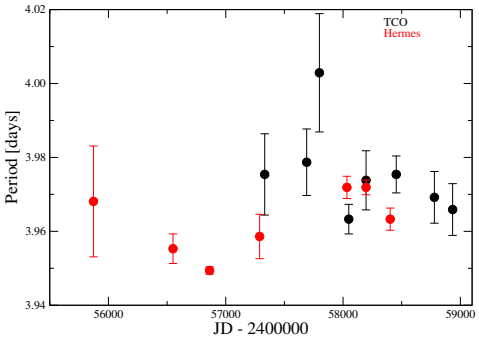

Figure 5: Polaris pulsational period changes in 2011–2020: red circles – Anderson (2019), black circles – our data.

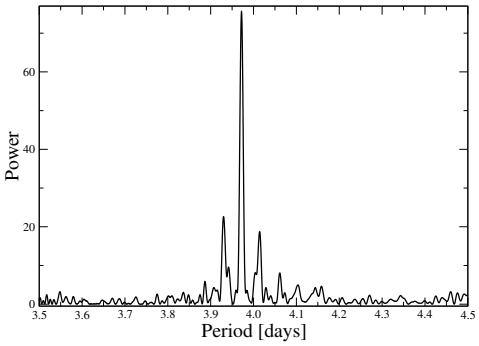

Figure 6: Fourier power spectrum of the Polaris Aa RV measurements for the 2015 – 2020 data.

constant pulsational period of 3.976±0.012 days (see Table 2). Anderson's data suggest a different value, because they were obtained on the ascending branch of the RV curve when the orbital velocity was significantly changing.

As seen in Fig. 7, the pulsational amplitude behaviour shows very noticeable changes during the time of our and Anderson's observations. Our errors are somewhat higher because of a lower spectral resolving power and longer periods of pulsational cycles averaging. Two vertical lines denote the moments of the periastron passage according to Anderson (2019) (violet) and Kamper (1996) (blue). As seen, the pulsational amplitude growth could be connected immediately to the orbital motion of Polaris Ab and its passing through periastron. Moreover, we can predict a further decrease of Polaris Aa pulsational amplitude in the nearest future according to this graph.

4. Effective temperature changes

Figure 8 demonstrates the mean $T_{\rm eff}$ values estimated spectroscopically for each of our observational season jointly with earlier specroscopic and photometrical ones. As seen, the mean $T_{\rm eff}$ of Polaris Aa during the last five years has been growing, and

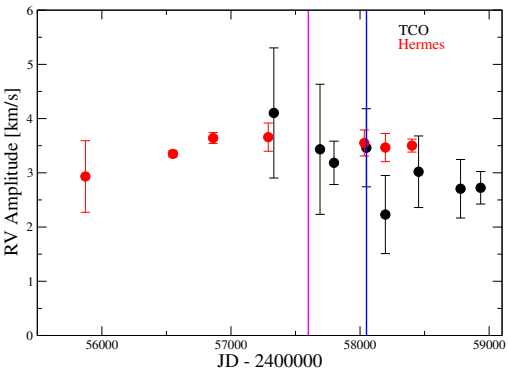

Figure 7: Pulsational amplitude of Polaris Aa according to data from Anderson (2019) (red) and our data from 2015 to 2020 (black). The violet and blue lines represent the moments of the periastron passage according to Anderson (2019) and Kamper (1996), respectively.

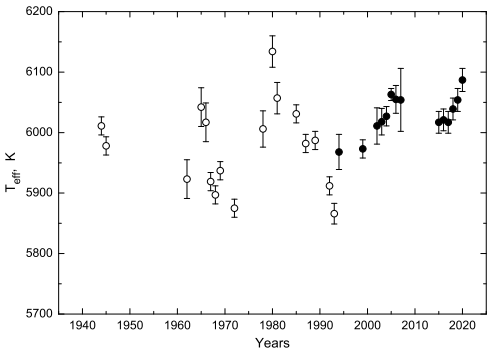

Figure 8: Variations of the mean $T_{\rm eff}$ of Polaris Aa during the last 75 years. Open circles - values from the $(B-V)$ vs. $T_{\rm eff}$ relationship by Gray (1992), filled circles - values from lines depth ratios (Kovtyukh 2007).

this phenomenon could be connected with the orbital motion of Polaris Ab.

5. Conclusions

The results of using 2585 RV data points during last 130 years we can suggest the following:

1. Our 187 *RV* observations obtained during last five years (8 observational seasons) along with 164 *RV* data points published by Anderson (2019) covered a fragment of the Polaris A orbit, which contained passages through a periastron and an ascending node.

2. The mean $T_{\rm eff}$ of Polaris Aa per season shows a gradual growth.

3. To check the influence of the Polaris Ab orbital motion on the Polaris Aa pulsational amplitude,

RV measurements from our data, those published by Anderson (2019), and some other sources have been analyzed.

4. Using these data, the orbit of the Polaris A binary system has been determined.

5. The mean pulsational period during five years demonstrates a certain stability.

6. The pulsational amplitude of Polaris Aa shows very strong changes, which contain a growth before HJD 2457350 with a subsequent decline. It is interesting that the decline has begun before the periastron passage.

7. Judging from the pulsational amplitude behaviour, we can predict its further decrease in the nearest future. Therefore further Polaris A *RV* observations are essential.

8. Orbital motion of Polaris Ab has an influence on the Polaris Aa pulsational amplitude depending on the orbital phase.

References

Anderson R.I.: 2019, *A&A*, **623**, A146.
Evans N.R., Karovska M., Bond H.E., Schaefer G.H., Sabu K.C., Mack J., Nelan E.P., Gallenne A. & Tingle E.D.: 2018, *ApJ*, **863**, 187.
Gray D.: 1992, *Observations and Analysis of Stellar Atmospheres, 2nd edn. Cambrige Univ. Press, Cambrige*
Kamper K.W.: 1996, *JRASC*, **90**, 140.
Kovtyukh V.V.: 2007, *MNRAS*, **378**, 617.
Roemer E.: 1965, *ApJ*, **141**, 1415.
Usenko I.A., Kovtyukh V.V., Miroshnichenko A.S., Danford S.: 2016, *Odessa Astron. Publ.*, **29**, 100.
Usenko I.A., Kovtyukh V.V., Miroshnichenko A.S., Danford S.: 2017, *Odessa Astron. Publ.*, **30**, 146.
Usenko I.A., Kovtyukh V.V., Miroshnichenko A.S., Danford S.: 2018, *MNRAS*, **481**, L115.